DOI: 10.1002/ange.201106243

Biofuels

Towards Quantitative Conversion of Microalgae Oil to Diesel-Range Alkanes with Bifunctional Catalysts**

*Baoxiang Peng, Yuan Yao, Chen Zhao, and Johannes A. Lercher**

Efficient conversion of biomass such as polysaccharides,[1] lignin,[2] and triglycerides[3] to biofuels has attracted considerable attention. Microalgae are being considered in that context as a promising renewable energy resource, having high triglyceride contents (up to 60 wt%)[4] and rapid growth rates that are 10–200 times faster than terrestrial oil crops such as soybean and rapeseed without directly competing with edible food/oil production.[5]

Currently, three approaches are used for microalgae oil refining. The first technique involves transesterification of triglycerides and alcohol into fatty acid alkyl esters (FAAEs) and glycerol, which is applied in the first-generation biodiesel production. Such esters, however, have a relatively high oxygen content and poor flow property at low temperatures, limiting their application as high-grade fuels.[6] The second technique employs the conventional hydrotreating catalysts, for example, sulfided NiMo and CoMo, for upgrading.[7] However, these sulfide catalysts contaminate products through sulfur leaching, and deactivate because of its removal from the surface by a reverse Mars–van Krevelen mechanism.[8] The third technique relies on supported noble and base metal catalysts for decarboxylation and decarbonylation of carboxylic acids to alkanes at 300–330 °C,[9] but these catalysts showed low activities and selectivities for C_{15}–C_{18} alkanes when triglycerides were converted, and the performance was only somewhat improved by a Pt-Re/ZSM-5 catalyst.[10] Contributions addressing microalgae oil upgrading using sulfur-free catalysts have not been reported. Herein, we report for the first time a novel and scalable catalyst, that is, Ni supported on and in zeolite HBeta, to quantitatively convert crude microalgae oil under mild conditions (260 °C, 40 bar H_2) to diesel-range alkanes as high-grade second-generation transportation biofuels.

Microalgae oil mainly consists of neutral lipids such as mono-, di-, and triglyceride. The microalgae oil (provided by Verfahrenstechnik Schwedt GmbH) used for this work consists of unsaturated C_{18} fatty acids (88.4 wt%), saturated C_{18} fatty acids (4.4 wt%), as well as some other C_{14}, C_{16}, C_{20}, C_{22}, and C_{24} fatty acids (7.1 wt% in total; see Table S1 in the Supporting Information).

[*] B. Peng, Y. Yao, Dr. C. Zhao, Prof. Dr. J. A. Lercher
Catalysis Research Center and Department of Chemistry
Technische Universität München
85747 Garching (Germany)
E-mail: johannes.lercher@ch.tum.de

[**] This work was supported by the EADS Deutschland GmbH.
Supporting information for this article is available on the WWW under http://dx.doi.org/10.1002/anie.201106243.

Without any purification, the crude microalgae oil was directly hydrotreated in batch mode with 10 wt% Ni/HBeta (Si/Al = 180) at 260 °C and 40 bar H_2 (see Figure 1). After 8 h reaction time, we obtained 78 wt% yield of liquid alkanes

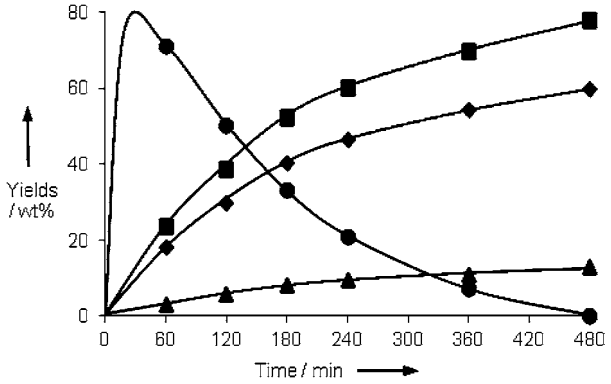

Figure 1. Product distributions for the transformation of microalgae oil over 10 wt% Ni/HBeta at 260 °C as a function of time, total liquid alkanes yield (■), octadecane yield (◆), heptadecane yield (▲), and stearic acid yield (●). Reaction conditions: microalgae oil (1.0 g), 10 wt% Ni/HBeta (Si/Al = 180, 0.2 g), dodecane (100 mL), 40 bar H_2 (reaction temperature), and stirring at 600 rpm.

(containing 60 wt% yield of C_{18} octadecane), which was very close to the theoretical maximum liquid hydrocarbon yield of 84 wt%. Propane (3.6 wt%) and methane (0.6 wt%) were the main products in the vapor phase. The metal leaching after reaction was detected below the atomic absorption spectroscopy (AAS) detection limit (1 ppm). Figure 1 shows that saturated fatty acids were the primary products for microalgae oil conversion, that is, the yield of stearic acid exceeded 70 wt% within 1 h. Then, the yield of saturated fatty acids gradually decreased accompanied with an increase in alkane yields (mainly including C_{18} and C_{17} alkanes) as a function of time. When microalgae oil is converted over the Ni/HBeta catalyst, 1) the hydrogenation of double bonds in the alkyl chain occurs very fast, 2) the slower hydrogenolysis of saturated triglycerides readily produces fatty acids and propane as initial primary products, and 3) the following hydrodeoxygenation of fatty acids to alkanes is the slowest (rate-determining) step in the overall reaction.

Variations of temperature and H_2 pressure showed that an increase of temperature from 250 to 270 °C at 40 bar enhanced the liquid alkane yield from 68 to 78 wt%, and an increase of the hydrogen pressure from 15 to 60 bar at 260 °C led to a decrease of *n*-C_{17} and *iso*-C_{18} yields from 28 to

11 wt%, whereas the *n*-C_{18} yield increased from 23 to 61 wt% (see Table S2 in the Supporting Information).

The upgrading of crude microalgae oil was also tested in a continuous flow system with a trickle bed reactor using 10 wt% Ni/HBeta catalysts under identical conditions (260°C, 40 bar H_2; see the Supporting Information). The results obtained from a continuous flow reactor were almost identical to those from a slurry batch reactor, in which the yield of C_{18} octadecane attained was 60 wt% and the total liquid alkane yield reached 78 wt%. The catalyst showed high activity and good stability during 120 h of testing (see Figure S2 in the Supporting Information). The catalyst productivity after 120 h was 78 g of algae oil per gram of catalyst.

To better understand the hydrodeoxygenation step of fatty acids to alkanes, the representative intermediate, stearic acid, was selected for further studies. Two types of acidic zeolite supports (HZSM-5 and HBeta) with Si/Al ratios of 45, 75, 120, 180, and 200 were explored. Ni nanoclusters supported on these zeolite catalysts were prepared by the incipient wetness impregnation method with metal loadings of 5 or 10 wt%, and characterized by N_2 sorption of the BET surface area, XRD for metal sites, and temperature-programmed desorption (TPD) of ammonia for acid sites (see Table 1 and the Supporting Information). The apparent specific surface areas of HZSM-5- and HBeta-supported Ni catalysts were approximately 300 and 550 $m^2 g^{-1}$, respectively. The average Ni particle sizes were about 15–30 nm calculated from XRD patterns by the Scherrer equation. As expected a higher Si/Al ratio or higher Ni content led to a lower acid site concentration of HZSM-5- and HBeta-based catalysts. The latter trend indicates that some Ni remained stabilized at the ion exchange sites also after reduction of the catalyst.

Full conversion of stearic acid was obtained with Ni/HZSM-5 (10 wt%, Si/Al = 45, acid density = 0.321 mmol g^{-1}) at 260°C in the presence of 40 bar H_2, but severe cracking of the produced alkanes (43% selectivity) was observed (see Table 1). By using HZSM-5-supported Ni catalysts with higher Si/Al ratios of 120 and 200 having lower acid site concentrations of 0.089 and 0.047 mmol g^{-1}, cracking was gradually suppressed, and the selectivity to C_{17} and C_{18} alkanes increased to 84 and 93%, respectively.

The Ni/HBeta catalyst (5 wt%, Si/Al = 75) led to a 96% conversion of stearic acid with selectivities of 82% for the C_{18} alkanes and of 18% for the C_{17} alkanes, almost eliminating the cracking of hydrocarbon chains. The HBeta catalyst with a higher Ni content (10 wt%, Si/Al = 75) displayed a similar activity as the former catalyst, but showed a lower selectivity to isomerized alkanes, indicating that its lower acid site concentration causes a lower isomerization rate. The Ni/HBeta catalyst with a higher Si/Al ratio of 180 led to quantitative conversion with about 90% C_{18} alkane selectivity, showing high atom economy. We speculate at present that the higher degree of cracking with Ni/HZSM-5 compared to Ni/HBeta is caused by a higher effective residence time caused by the higher Brønsted acid site concentration and the narrower pores in the HZSM-5 zeolite. The peaks in the TPD of ammonia indicate very similar strength of acid sides in both materials (see Figure S4 in the Supporting Information). To explore the potential to higher C_{18} alkane yields and lower cracking yields, Ni/HBeta (10 wt%, Si/Al = 180) was chosen for a detailed kinetic study.

With Ni/HBeta (10 wt%, Si/Al = 180), less than 10% C_{17} *n*-heptadecane and more than 90% C_{18} octadecane were formed at nearly complete conversion of stearic acid at 260°C as seen in Figure 2a. The intermediates octadecanal (concentration < 0.02%) and 1-octadecanol (concentration < 0.1%) were only observed in traces. This suggests that stearic acid is hydrogenated with a slow rate to octadecanal in the first step, and then rapidly reduced to 1-octadecanol, and followed by rapid dehydration–hydrogenation reactions, producing the C_{18} alkane as the final product. The presence of the intermediates also shows that the hydrogenation–deoxygenation reactions are the main route for producing C_{18} alkanes without carbon loss (90% selectivity), whereas the decarbonylation of the intermediately formed C_{18} aldehyde is the minor route.

To verify this hypothesis, the kinetics of the intermediate product 1-octadecanol was also studied with Ni/HBeta (10 wt% Ni, Si/Al = 180) under identical conditions (260°C and 40 bar H_2) (see Figure 2b). *n*-Octadecane (85% yield) and C_{17} *n*-heptadecane (5% yield) were the main products at 94% conversion. Distearyl ether was observed as intermediates through intermolecular dehydration of the C_{18} alcohol, but as the reaction proceeded, the ether was cleaved again and deoxygenated through elimination of water and hydrogenation of the alkene to *n*-octadecane. The dehydration product, *n*-octadecene, was not detected because of the fast

Table 1: Comparison of stearic acid conversion over Ni/zeolite catalysts at 260°C.[a]

Catalyst	Metal loading [wt%]	Si/Al [mol/mol]	BET surface area [$m^2 g^{-1}$]	Acid density [mmol g^{-1}][b]	$d_{Ni(111)}$ [nm][c]	$d_{Ni(200)}$ [nm][c]	Conversion [%]	Selectivity [C%] *n*-C_{18}	*iso*-C_{18}	*n*-C_{17}	*iso*-C_{17}	cracking
Ni/HZSM-5	10	45	279	0.321	28	24	100	41.1	6.3	9.2	0.4	42.7
Ni/HZSM-5	10	120	286	0.089	29	23	65	67.5	7.6	8.8	–	15.9
Ni/HZSM-5	10	200	304	0.047	30	24	60	80.1	6.3	6.1	–	7.2
Ni/HBeta	5	75	603	0.188	20	15	96	66.5	15.0	13.8	3.8	0.7
Ni/HBeta	10	75	586	0.171	25	20	100	72.6	10.1	14.8	1.6	0.6
Ni/HBeta	5	180	565	0.069	21	18	96	82.8	6.0	10.2	0.2	0.4
Ni/HBeta	10	180	523	0.053	25	20	98	84.6	5.2	9.5	–	0.4

[a] Reaction conditions: stearic acid (1.0 g), dodecane (100 mL), Ni/zeolite (0.2 g), H_2 (40 bar at 260°C), 8 h, and stirring at 600 rpm. [b] Determined by TPD of ammonia. [c] Calculated from XRD by the Scherrer equation.

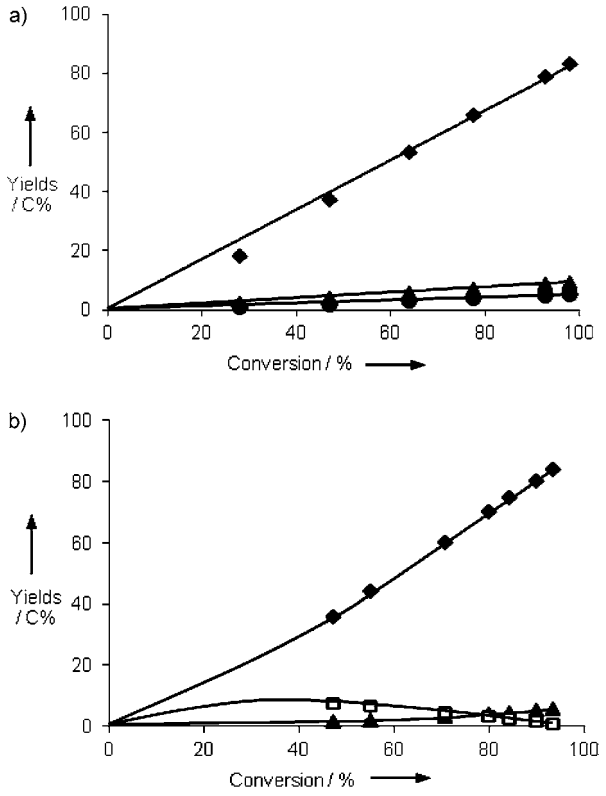

Figure 2. a) Yields of *n*-octadecane (◆), *n*-heptadecane (▲), and *iso*-octadecane (●) as a function of stearic acid conversion. b) Yield of *n*-octadecane (◆), *n*-heptadecane (▲), and distearyl ether (□) as a function of 1-octadecanol conversion. Reaction conditions: a) stearic acid (1.0 g), 10 wt% Ni/HBeta (Si/Al = 180, 0.2 g); b) 1-octadecanol (1.0 g), and 10 wt% Ni/HBeta (Si/Al = 180, 0.05 g); dodecane (100 mL), 260 °C, 40 bar H_2 (reaction temperature), 8 h, and stirring at 600 rpm.

hydrogenation of the double bond. This allows us to estimate that the dehydration rate of 1-octadecanol (8.6 mmol g^{-1} h^{-1}) is around four times faster than the hydrogenation rate of stearic acid (2.2 mmol g^{-1} h^{-1}), which explains that only the trace amounts of 1-octadecanol and octadecanal are observed during the conversion of stearic acid. We conclude therefore that the Ni-catalyzed hydrogenation is the rate-determining step in the overall reaction. In addition, based on our previous experiments with 1- and 2-propanol,[11] we infer that C_{17} *n*-heptadecane is produced by metal-catalyzed decarbonylation of *n*-octadecanal, producing also 1 mol of CO. In addition, the 1-octadecanol and octadecanal are concluded to be equilibrated because the yields of individually produced *n*-C_{17} and *n*-C_{18} alkanes increased linearly with increasing conversion (see Figure 2a).

The impacts of reaction temperature and pressure on the conversion of stearic acid with 10 wt% Ni/HBeta are documented in Figures S5 and S6 in the Supporting Information. With increasing reaction temperature from 250 to 270 °C, the yields of C_{17} *n*-heptadecane and C_{18} *iso*-octadecane increased from 10 to 20%, but the yield of C_{18} *n*-octadecane was comparable (80%), indicating a higher increase of the rates of decarbonylation and isomerization. As the conversion was high in all three experiments, we infer that the effect is either related to a longer contact time of the intermediates (produced in larger concentrations) or a higher apparent activation energy of the decarbonylation of the aldehyde and the isomerization of the alkane compared to the hydrogenation of stearic acid. Figure S6 in the Supporting Information also shows that the increase of the H_2 pressure from 15 to 60 bar led to an increase of the C_{18} *n*-octadecane yield from 65 to 84% after 8 h, whereas the lower hydrogen pressure (15 bar) favored not only decarbonylation (C_{17} *n*-heptadecane, 15%), but also C_{18} *iso*-octadecane (15%) formation. This is related to the fact that the higher hydrogen pressure benefits the fatty acid hydrogenation step (rate-determining step) and shifts the equilibrium from octadecanal to 1-octadecanol, and thus, the overall hydrodeoxygenation rate and the selectivity to C_{18} *n*-octadecane are enhanced, whereas the selectivities to C_{17} *n*-heptadecane and C_{18} *iso*-octadecane are suppressed.

Combining these experiments allows to formulate the overall reaction pathway for microalgae oil transformation (see Scheme 1). The reaction pathway proceeds through an initial metal-catalyzed hydrogenation of double bonds in the alkyl chain, followed by hydrogenolysis of the formed saturated triglyceride leading to fatty acid and propane. The subsequent hydrogenation of the carboxylic group of fatty acid leads to the corresponding aldehyde, for example, octadecanal (rate-determining step), followed by either decarbonylation of octadecanal to *n*-heptadecane and carbon monoxide (minor route) or hydrogenation of octadecanal to 1-octadecanol (major route). Subsequently, the produced 1-octadecanol undergoes sequential acid-catalyzed dehydration and metal-catalyzed hydrogenation leading to the final *n*-octadecane. An abundance of acidic sites in the zeolite leads to hydroisomerization and hydrocracking of the alkanes. CO may react with H_2 to produce methane and water.

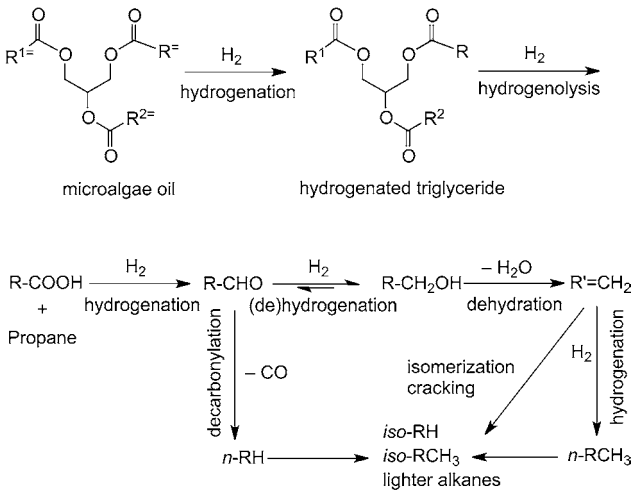

$R^{1=}$, $R^{2=}$, $R^{=}$: unsaturated alkyl chain

Methanation: $CO + H_2 = CH_4 + H_2O$

Scheme 1. Proposed reaction pathway for transformation of microalgae oil to alkanes over bifunctional Ni/HBeta catalysts.

In summary, we have shown that microalgae oil can be nearly quantitatively hydrodeoxygenated to alkanes by cascade reactions on bifunctional catalysts based on Ni and an acidic zeolite. Ni catalyzes efficiently the hydrogenolysis of the fatty acid ester, the decarbonylation of aldehyde intermediates, as well as the hydrogenation of −COOH, −CHO and C=C double bonds in reactants and intermediates. The acid function catalyzes the dehydration of alcohol intermediates and the hydroisomerization and hydrocracking of the alkane products. The knowledge of the individual reaction rates allows balancing these rates by adjusting the concentration of catalytically active sites to design tailored and stable catalysts for selectively converting crude microalgae oil to diesel-range alkanes. The approach opens new possibilities to produce sulfur-free high-grade green transportation fuels from microalgae at large scale.

Experimental Section

Ni nanoclusters supported on zeolites (HZSM-5 samples and HBeta with a Si/Al ratio of 75 obtained from Süd-Chemie AG München, HBeta with a Si/Al ratio of 180 obtained from Zeolyst) were prepared by the wetness impregnation method. The typical experiments with microalgae oil, stearic acid, or 1-octadecanol were carried out as follows: reactant (1.0 g), dodecane (100 mL), and Ni/zeolite (0.2 g) were charged into a batch autoclave (Parr Instrument, 300 mL). Then the autoclave was purged with N_2 at ambient temperature, and the gas was changed to H_2, and the reaction mixture was stirred until the required temperature was reached. The reaction was carried out at 260 °C, 40 bar H_2 (reaction temperature), and stirring at 600 rpm for 8 h. The products in the gas phase were analyzed online by gas chromatograph (GC) with a thermal conductivity detector (TCD) and two capillary columns (MS-5A and HP-Plot Q). Liquid samples were manually collected during the run and analyzed by GC/GC-MS equipped with FID detector and a HP-5 column. The internal standard (eicosane) was used for quantification of the liquid products.

The conversion is given as weight of converted reactant per weight of the starting reactant multiplied by 100 %. The yield in [C %] is defined as C atoms in each product per C atoms in the starting reactant multiplied by 100 %. The yield in [wt %] is given as weight of each product per weight of the starting reactant multiplied by 100 %.

Received: September 3, 2011
Revised: October 19, 2011
Published online: November 15, 2011

Keywords: green chemistry · hydrogenolysis · supported catalysts · zeolites

[1] a) G. W. Huber, J. N. Chheda, C. J. Barrett, J. A. Dumesic, *Science* **2005**, *308*, 1446 – 1450; b) J. Q. Bond, D. M. Alonso, D. Wang, R. M. West, J. A. Dumesic, *Science* **2010**, *327*, 1110 – 1114; c) J. P. Lange, R. Price, P. M. Ayoub, J. Louis, L. Petrus, L. Clarke, H. Gosselink, *Angew. Chem.* **2010**, *122*, 4581 – 4585; *Angew. Chem. Int. Ed.* **2010**, *49*, 4479 – 4483.

[2] a) C. Zhao, Y. Kou, A. A. Lemonidou, X. Li, J. A. Lercher, *Angew. Chem.* **2009**, *121*, 4047 – 4050; *Angew. Chem. Int. Ed.* **2009**, *48*, 3987 – 3990; b) C. Zhao, Y. Kou, A. A. Lemonidou, X. Li, J. A. Lercher, *Chem. Commun.* **2010**, *46*, 412 – 414; c) N. Yan, Y. Yuan, R. Dykeman, Y. Kou, P. J. Dyson, *Angew. Chem.* **2010**, *122*, 5681 – 5685; *Angew. Chem. Int. Ed.* **2010**, *49*, 5549 – 5553; d) C. Zhao, J. He, A. A. Lemonidou, X. Li, J. A. Lercher, *J. Catal.* **2011**, *280*, 8 – 16.

[3] a) F. R. Ma, M. A. Hanna, *Bioresour. Technol.* **1999**, *70*, 1 – 15; b) B. X. Peng, Q. Shu, J. F. Wang, G. R. Wang, D. Z. Wang, M. H. Han, *Process Saf. Environ. Prot.* **2008**, *86*, 441 – 447.

[4] a) P. M. Schenk, S. R. Thomas-Hall, E. Stephens, U. C. Marx, J. H. Mussgnug, C. Posten, O. Kruse, B. Hankamer, *Bioenerg. Res.* **2008**, *1*, 20 – 43; b) T. M. Mata, A. A. Martins, N. S. Caetano, *Renewable Sustainable Energy Rev.* **2010**, *14*, 217 – 232.

[5] a) G. W. Huber, S. Iborra, A. Corma, *Chem. Rev.* **2006**, *106*, 4044 – 4098; b) Y. Chisti, *Biotechnol. Adv.* **2007**, *25*, 294 – 306.

[6] P. Šimácek, D. Kubicka, G. Šebor, M. Pospíšil, *Fuel* **2009**, *88*, 456 – 460.

[7] a) G. W. Huber, P. O'Connor, A. Corma, *Appl. Catal. A* **2007**, *329*, 120 – 129; b) R. Kumar, B. S. Rana, R. Wiwari, E. Verma, R. Kumar, R. K. Joshi, M. O. Garg, A. K. Sinha, *Green Chem.* **2010**, *12*, 2232 – 2239; c) R. Sotelo-Boyás, Y. Y. Liu, T. Minowa, *Ind. Eng. Chem. Res.* **2011**, *50*, 2791 – 2799.

[8] a) E. Laurent, B. Delmon, *J. Catal.* **1994**, *146*, 281 – 291; b) T. R. Viljava, R. S. Komulanien, A. O. I. Krause, *Catal. Today* **2000**, *60*, 83 – 92.

[9] a) M. Snåre, I. Kubičková, P. Mäki-Arvela, K. Eränen, D. Y. Murzin, *Ind. Eng. Chem. Res.* **2006**, *45*, 5708 – 5715; b) M. Snåre, I. Kubičková, P. Mäki-Arvela, D. Chichova, K. Eränen, D. Yu. Murzin, *Fuel* **2008**, *87*, 933 – 945; c) J. G. Immer, M. J. Kelly, H. H. Lamb, *Appl. Catal. A* **2010**, *375*, 134 – 139; d) W. F. Maier, W. Roth, I. Thies, P. v. R. Schleyer, *Chem. Ber.* **1982**, *115*, 808 – 812.

[10] a) I. Kubičková, M. Snåre, K. Eränen, P. Mäki-Arvela, D. Yu. Murzin, *Catal. Today* **2005**, *106*, 197 – 200; b) K. Murata, Y. Liu, M. Inaba, I. Takahara, *Energy Fuels* **2010**, *24*, 2404 – 2409.

[11] A. Wawrzetz, B. Peng, A. Hrabar, A. Jentys, A. A. Lemonidou, J. A. Lercher, *J. Catal.* **2010**, *269*, 411 – 420.

